

This article was downloaded by: [Tomsk State University of Control Systems and Radio]

On: 23 February 2013, At: 07:18

Publisher: Taylor & Francis

Informa Ltd Registered in England and Wales Registered Number: 1072954

Registered office: Mortimer House, 37-41 Mortimer Street, London W1T 3JH, UK



Molecular Crystals and Liquid Crystals

Publication details, including instructions for authors and subscription information:

<http://www.tandfonline.com/loi/gmcl16>

Ultrasonic Absorption and Dispersion in Cholesteryl Esters

J. F. Dyro^a & P. D. Edmonds^{b c}

^a Emergency Care Research Institute, 913 Walnut St., Philadelphia, PA, 19107

^b The Institute of Electrical and Electronics Engineers, Inc., 345 E. 47th St., New York, 10017

^c Department of Biomedical Electronic Engineering, Moore School of Electrical Engineering University of Pennsylvania, Philadelphia, Pennsylvania, 19104, U.S.A.

Version of record first published: 21 Mar 2007.

To cite this article: J. F. Dyro & P. D. Edmonds (1974): Ultrasonic Absorption and Dispersion in Cholesteryl Esters, *Molecular Crystals and Liquid Crystals*, 25:1-2, 175-193

To link to this article: <http://dx.doi.org/10.1080/15421407408083416>

PLEASE SCROLL DOWN FOR ARTICLE

Full terms and conditions of use: <http://www.tandfonline.com/page/terms-and-conditions>

This article may be used for research, teaching, and private study purposes. Any substantial or systematic reproduction, redistribution, reselling, loan, sub-licensing, systematic supply, or distribution in any form to anyone is expressly forbidden.

The publisher does not give any warranty express or implied or make any representation that the contents will be complete or accurate or up to date. The accuracy of any instructions, formulae, and drug doses should be independently verified with primary sources. The publisher shall not be liable for any loss, actions, claims, proceedings, demand, or costs or damages whatsoever or howsoever caused arising directly or indirectly in connection with or arising out of the use of this material.

Ultrasonic Absorption and Dispersion in Cholesteryl Esters

J. F. DYRO[†] and P. D. EDMONDS[‡]

*Department of Biomedical Electronic Engineering
Moore School of Electrical Engineering
University of Pennsylvania
Philadelphia, Pennsylvania, 19104, U.S.A.*

(Received August 16, 1973)

Propagation of ultrasonic longitudinal waves at frequencies from 10 to 70 MHz was studied in three 18-carbon unsaturated fatty acid esters of cholesterol-cholesteryl oleate (CO), cholesteryl linoleate (CL), and cholesteryl linolenate (CLn)—and three mixtures of the esters—80%CL-20%CO, 95%CL-5%CO, and 80%CLn-20%CO. The study was made in temperature ranges over which all systems exhibited the isotropic, cholesteric, and smectic states. Measurements of the ultrasonic attenuation coefficient and velocity of propagation of longitudinal waves were made by a variable pathlength pulse transmission technique. Density measurements as a function of temperature were also made.

Measurements of the attenuation coefficients indicate that the 10 to 70 MHz frequency range lies at the high end of a relaxation region whose characteristic frequency is below 10 MHz. No anomalous behaviour of either the longitudinal attenuation coefficient or propagation velocity in the vicinity of isotropic-cholesteric or cholesteric-smectic phase transitions was observed. The frequency dependence of the absorption parameter, α/f^2 , where α is the attenuation coefficient and f is the frequency, is consistent with the dependence reported by Zvereva and Kapustin on the similar, but smaller, molecule of cholesteryl caprate. The temperature dependence of bulk and shear viscosities indicates that both structural and thermal relaxation occur in all systems over the temperature and frequency range studied.

[†] Present address — Emergency Care Research Institute, 913 Walnut St., Philadelphia, PA 19107.

[‡] Present address — The Institute of Electrical and Electronics Engineers, Inc., 345 E. 47th St., New York, NY 10017.

INTRODUCTION

The absorption and dispersion of ultrasound in three cholesteryl esters and their mixtures using a pulse transmission technique are reported. This work, together with an investigation of the dynamic viscoelastic properties of the same esters¹ enables their more complete physical characterization. Of particular importance is the system, CO-CL, found in high proportions in some diseased human tissue, which undergoes a cholesteric-isotropic transition at body temperature.

The propagation of longitudinal ultrasonic waves in a viscoelastic medium was described by Edmonds and Orr.² Two quantities are measured: the absorption coefficient α and the velocity v .

According to classical theory the absorption of sound can be attributed largely to the viscous resistance offered to the displacement of element volumes of fluid by the sound pressure wave. However, in the systems studied here the most significant additional contribution to attenuation probably arises from the coupling of the energy of the sound wave with time dependent molecular processes, or relaxational processes.

Relaxational processes may be divided into the two main categories, thermal and structural. In the thermal case, the sound wave perturbs the medium directly by a change in temperature accompanying a change in volume. In the structural case, the volume change of the wave changes the pressure which directly effects the medium. The thermal mechanism of sound absorption is due to the rise in temperature accompanying an adiabatic compression of a medium with $\gamma \neq 1$ and to the time lag for transfer of energy from external to internal degrees of freedom†. For nonassociated and nonpolar liquids, the thermal relaxation theory has been quite successful in explaining sound absorption.

All thermal relaxation processes observed so far can be described by the equation $\alpha/f^2 = A/[(1 + (f/f_c)^2)] + B$ where A is a parameter of the time dependent process, B is the classical, viscous, absorption and f_c is the single characteristic frequency.

Structural mechanisms usually, but not always, can be characterized by a distribution of relaxation frequencies. Structural relaxation effects due directly to the volume change and not the temperature change, predominate for associated liquids and polymeric liquids in which large intermolecular forces exist. On the molecular level of the lattice theory of liquids, the acoustic pressure causes the molecules of a liquid to jump into vacant lattice positions. This structural rearrangement takes a finite amount of time causing the volume changes to be

† γ is the ratio of specific heats, C_p/C_v , where C_p and C_v are the specific heats at constant pressure and volume, respectively.

out of phase with the pressure. The pressure (and temperature) variations cause changes in the degree of order present in a liquid. The more the liquid is compressed the closer the packing and the higher the density of the occupied lattice site. An increase of temperature causes expansion of the lattice and reduction in the density of occupied lattice sites. Sound pressure and temperature variations therefore work in opposition in inducing changes in liquid structure. By studying the temperature and frequency dependence of the attenuation coefficient, an understanding of the mechanisms of absorption may be gained. Long range ordering in the liquid crystalline state suggests the likelihood of structural relaxation mechanisms. In addition, thermal mechanisms may predominate in the vicinity of cholesteric-isotropic phase transitions.

EXPERIMENTAL

Sample preparation

CL and CLn of 99% purity and CO of >95% purity were purchased from Distillation Products Industries, Eastman Chemical, Rochester, N.Y. The esters were stored at 0°C under nitrogen. The mixing of samples, heating to the isotropic, and transfer to sample cell were all done under an atmosphere of high purity dry nitrogen. The sample cell was flushed with dry high purity nitrogen before the sample was introduced and a continuous stream of nitrogen was maintained thereafter. The temperature of the nitrogen was maintained to within 0.5°C of the sample temperature. At the start of a measurement run, a volume of about 25 grams were transferred to the ultrasonic measurement cell and about 3 grams were transferred to a test tube to be sealed under nitrogen and used as a control sample for transition temperature determination.

Temperature control and measurement

The sample was contained in the cell described previously³ and shown schematically in Figure 1. Water from a constant temperature bath is circulated through the annular space of the doubled walled cell. The bath is capable of maintaining temperature within the range of interest to better than 0.02°C. Since the measurement temperatures desired were about 20°C above room temperature, heat loss or thermal load on the temperature bath was minimized by enclosing the cell in an oven whose temperature was kept to within $\pm 1^\circ\text{C}$ of the bath temperature.

The temperature of the liquid sample was measured by means of a copper-constantan thermocouple pair with one junction mounted adjacent to the tip of

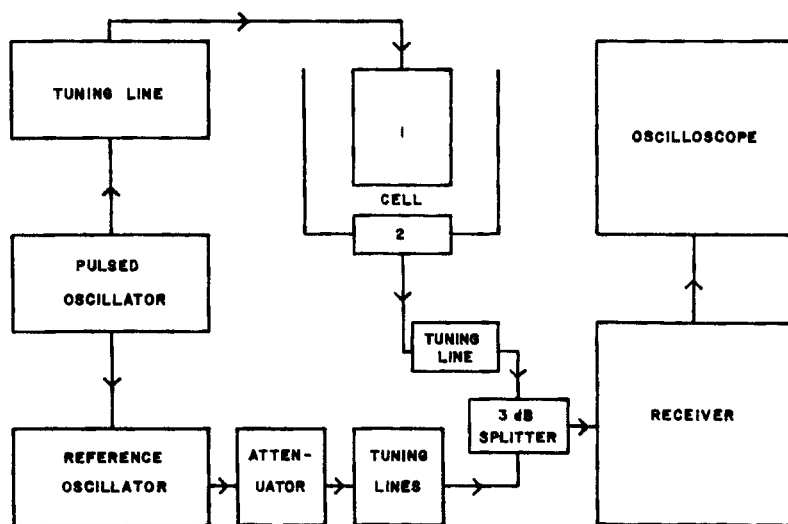


FIGURE 1 Block diagram of longitudinal wave apparatus (10–70 MHz).

the movable quartz rod and the other immersed in the bath liquid. The long term ($t > 60$ min) temperature instability of the sample is less than $\pm 0.025^\circ\text{C}$.

Instrumentation

Measurements of α are made by a variable path pulse transmission technique introduced by Pellam and Galt⁴. In Figure 1 a block diagram of the apparatus is shown. The pulsed oscillator (Arenberg Model PG-650C No. 348) provides a variable pulse length for a range of frequencies from 4.9 to 176 MHz. The high-frequency signal from the pulsed oscillator is supplied to an X-cut quartz crystal operating in the region of an odd harmonic of its fundamental frequency 10 MHz. The transducer is acoustically coupled with Dow Corning Resin 276-V9 to a fused quartz rod delay line (1). The delay line is rigidly clamped to a micrometer slide (Gaertner Scientific Corporation M342), which can be moved in a range of 10 cm vertically along the axis of the transducers. The micrometer can be read with an accuracy of 0.001 mm. The transmitted pulse impinges upon a quartz delay rod (2) which transmits the wave to an identical receiving transducer. The received pulse then goes through tuning lines and is combined with a reference signal by a 3dB splitter (Electronic Navigation Industries, Model PM 1202). The signals go to the receiver (RDO) and are then displayed on an oscilloscope (Tektronix 585A). The reference signal is provided by an oscillator (Hewlett-Packard 608D) which receives a variable delay trigger from the Arenberg pulsed oscillator. The reference oscillator includes an attenuator and has a

continuously variable output of 129 dB. The reference signal is passed through two step attenuators (Kay, Models 60-0 and 60-1) which have range of 0-60 dB in 10 dB steps and 0-10 dB in 1 dB steps, then through the tuning lines to the 3 dB splitter.

The velocity of propagation, v , is measured using the same apparatus as shown in Figure 1 by comparing the phase difference between the received pulse and a reference *CW* signal; these were made coherent by gating the pulsed oscillator with a *CW* signal from the reference oscillator. The sonic wavelength is equal to the distance between two successive maxima or minima of the received pulse amplitude corresponding to in phase or 180° out of phase conditions. The velocity can be calculated by taking the product of the wavelength and the frequency.

Uncertainties in α and v

The uncertainty in the absorption coefficient is determined by the precision with which the amplitude of the received pulse can be made equal to that of the comparison pulse by varying the ultrasonic path length and observing both received and comparison pulses on the oscilloscope screen. The overall uncertainty in α is $\pm 3\%$ based on a standard error of $\pm 1\%$. Systematic variations in temperature and frequency contribute $\pm 0.2\%$ to the overall uncertainty and are, therefore, considered negligible. The imprecision with which the micrometer scale can be read is negligible. No corrections for diffraction were found necessary.

The uncertainty in the longitudinal velocity is a function of the uncertainty in the determinations of wavelength, λ , and frequency, f , since $v = f\lambda$. An uncertainty in λ of $\pm 0.4\%$ for measurements at 10 MHz is based on a standard error of $\pm 0.1\%$ and a systematic error of $\pm 0.1\%$. The allowance of $\pm 0.1\%$ for systematic error results from the frequency drift of the *RF* pulse generator. The uncertainty in f determination based on imprecision and systematic error is negligible. Therefore, the overall uncertainty in v is $\pm 0.4\%$. As the measurement frequency increases, however, α increases as well, such that at 50 MHz only 20 minima can be read on the oscilloscope display against the background of noise and at 70 MHz barely 10 can be seen. Typically 40 to 50 wavelength minima can be read at 10 MHz. An uncertainty in velocity of $\pm 1.6\%$ can be expected at 70 MHz based on a standard error of $\pm 0.5\%$ and a $\pm 0.1\%$ systematic error.

Density measurement and uncertainty

Density measurements are made using a Reischauer Specific Gravity bottle with a 25 ml capacity. Esters obtained from Eastman are used in all density and falling ball viscosity measurements. The bottle is filled such that, when the

sample and bottle, placed in the bath, attain the highest measurement temperature, the meniscus appears at or just below the top graduation on the neck of the bottle. As the temperature of the bath is lowered the meniscus level is recorded. Measurements of ρ as a function of temperature have uncertainty of about $\pm 0.04\%$ in the isotropic phase and $\pm 0.08\%$ in the cholesteric and smectic states. The uncertainty in the isotropic phase of $\pm 0.04\%$ is based on a standard error of $\pm 0.01\%$ and a systematic error of $\pm 0.01\%$. The uncertainty in the cholesteric and smectic phases of $\pm 0.08\%$ is based on a standard error of $\pm 0.01\%$ and a systematic error of $\pm 0.05\%$. The increase in viscosity of the sample in the liquid crystalline states accounts for the increase in systematic error. Upon lowering the temperature of the density bottle, a portion of the highly viscous sample adheres to the neck of the measurement bottle. This results in a mass of sample below the meniscus which is less than the mass determined by weighing the difference in mass of the bottle with and without sample.

By selectively melting the sample with a heating gun to the isotropic state, much of the sample adhering to the neck can be reunited with the bulk of the sample below the meniscus. Some material still remains, however, and accounts for the additional systematic error in the density determination.

RESULTS

The following results are exhibited:

Density, ρ vs. T

- a. CO, CL and CLn (Figure 2);
- b. CO, 80% CL-20% CO, and CL (Figure 3);
- c. CO, 80% CLn-20% CO, and CLn (Figure 4).

Longitudinal wave, α/f^2 and ν vs. T and f

- a. CL: α/f^2 vs. T (Figure 5), ν vs. T (Figure 6); α/f^2 vs. f (Figure 7), and ν vs. f (Figure 8);
- b. CO, CL, and CLn; α/f^2 vs. T (Figure 9) and ν vs. T (Figure 10) at 10 MHz;
- c. CO, 80% CL-20% CO, 95% CL-5% CO, and CO; α/f^2 vs. T (Figure 11) and ν vs. T (Figure 12) at 10 MHz;
- d. CO, 80% CLn-20% CO, and CLn; α/f^2 vs. T (Figure 13) and ν vs. T (Figure 14) at 10 MHz.

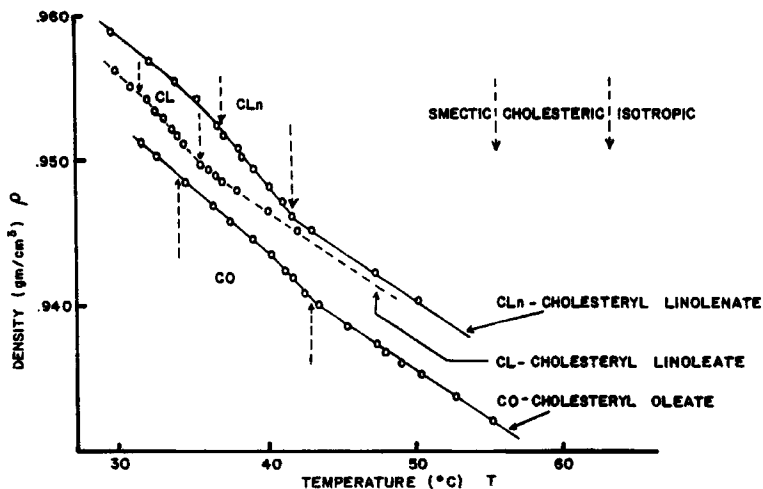


FIGURE 2 Density vs. temperature of CO, CL, and CLn.

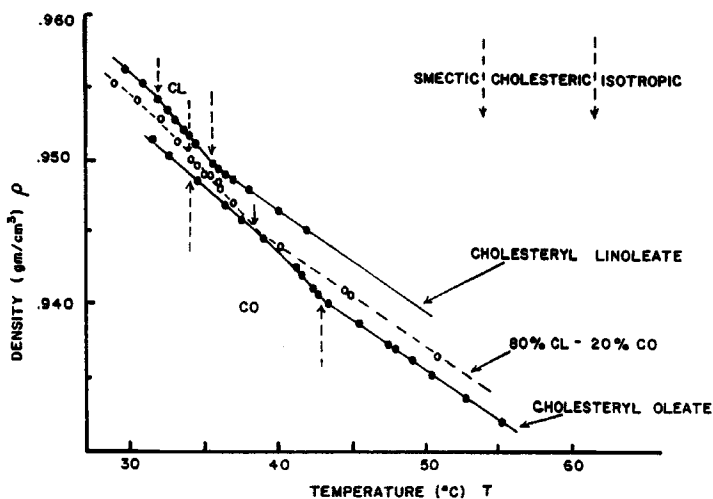


FIGURE 3 Density vs. temperature of CO, 80% CO-20% CO, and CL.

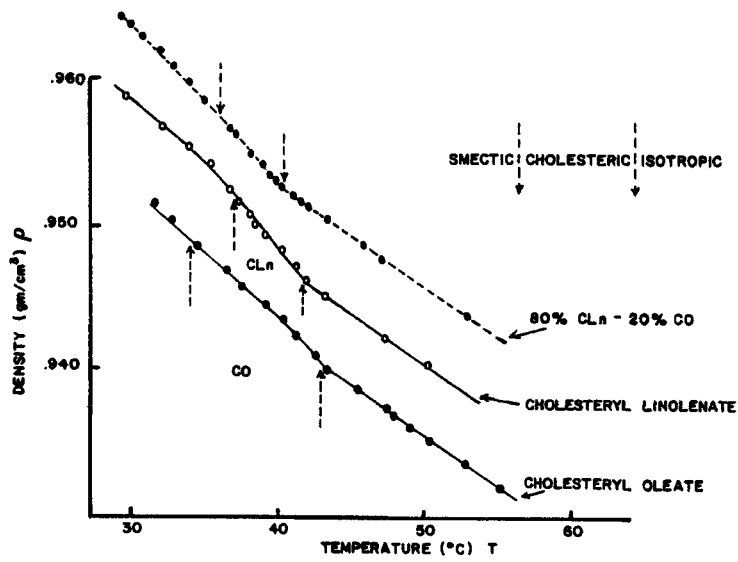


FIGURE 4 Density vs. temperature of CO, 80% CLn-20% CO and CLn.

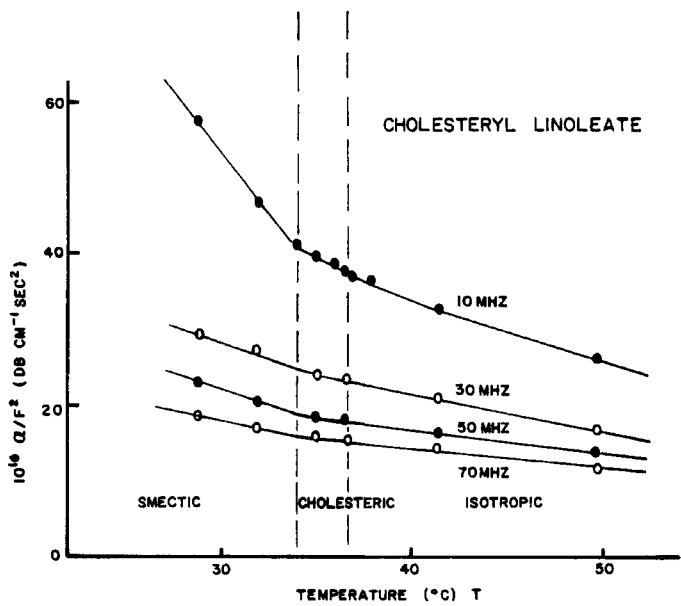


FIGURE 5 α/f^2 vs. temperature of CL at 10, 30, 50, and 70 MHz.

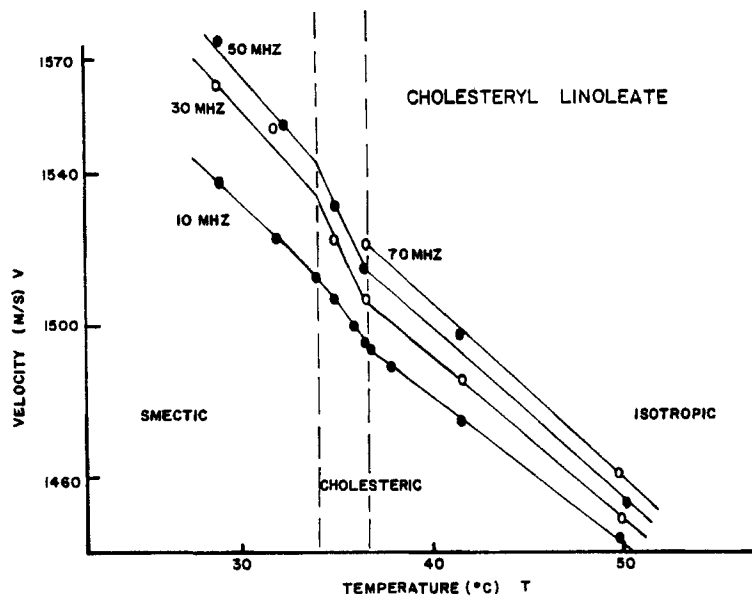
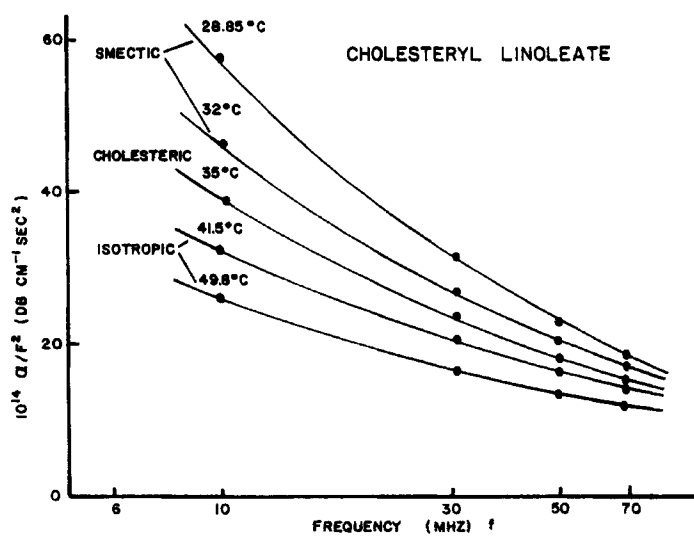


FIGURE 6 Velocity vs. temperature of CL at 10, 30, 50 and 70 MHz.

FIGURE 7 α/f^2 vs. frequency of CL at smectic, cholesteric, and isotropic temperatures.

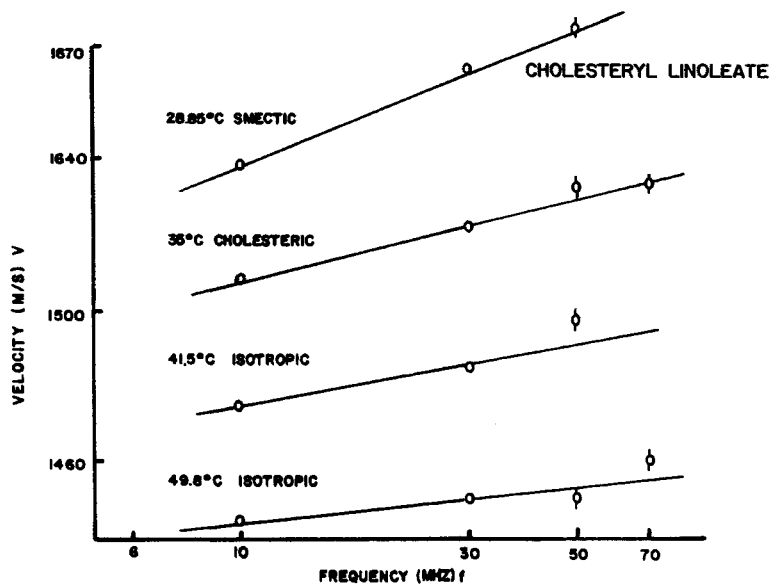


FIGURE 8 Velocity vs. frequency of CL at smectic, cholesteric, and isotropic temperatures.

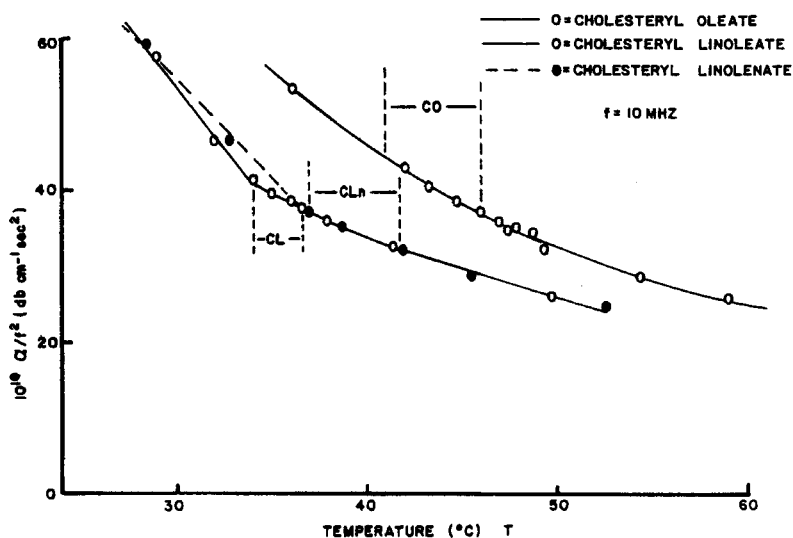


FIGURE 9 α/f^2 vs. temperature of CO, CL and CLn at 10 MHz.

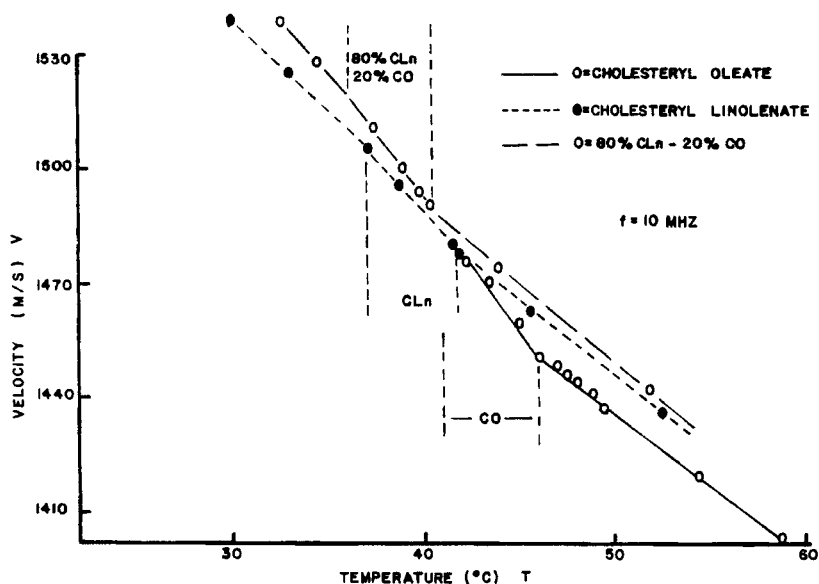
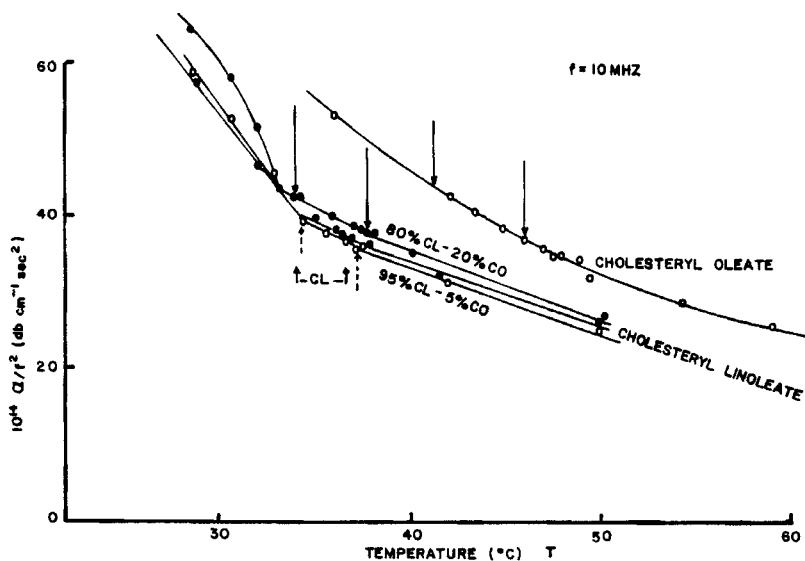


FIGURE 10 Velocity vs. temperature of CO, CL, and CLn at 10 MHz.

FIGURE 11 α/f^2 vs. temperature of CO, 80% CL-20%CO, 95%CO, and CL at 10 MHz.

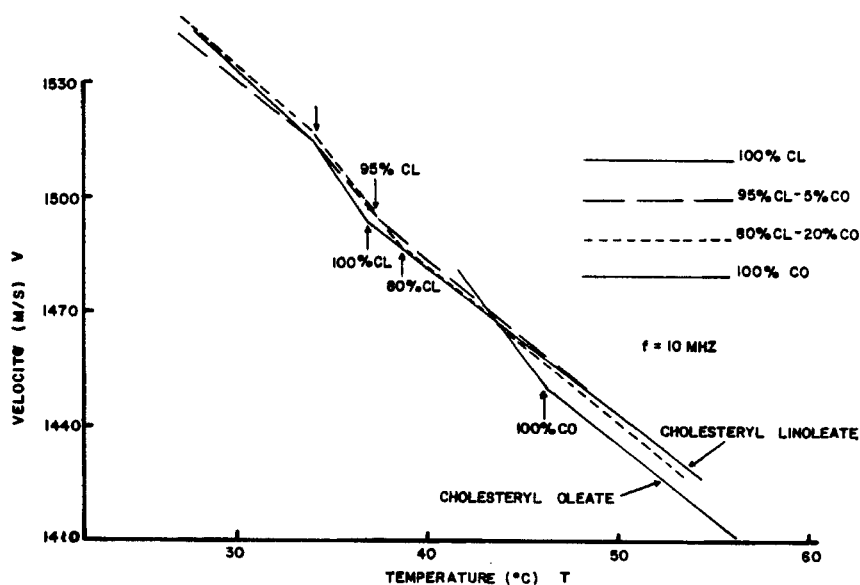


FIGURE 12 Velocity vs. temperature of CO, 80%CL-20% CL, 95% CL-5%CO, and CL at 10 MHz.

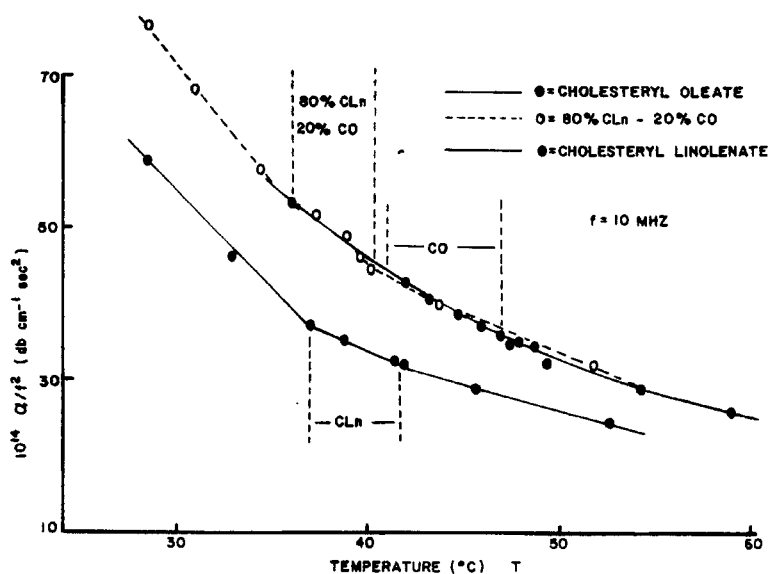


FIGURE 13 α/f^2 vs. temperature of CO, 80% CLn-20% CO, and CLn at 10 MHz.

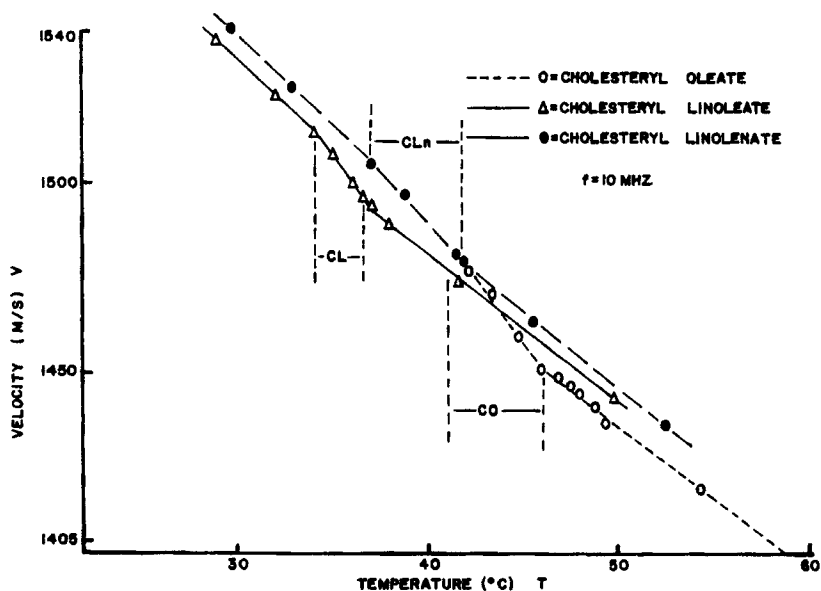


FIGURE 14 Velocity vs. temperature of CO, 80% CLn-20% CO, and CLn at 10 MHz.

CONCLUSIONS

Density

Increasing numbers of double bonds in the series CO, CL, and CLn correlate with increasing density. Comparing any one phase, the change in density with temperature is nearly equal for all three esters and for their mixtures shown in Figure 2, 3, and 4. The temperature coefficients of density in the isotropic, cholesteric, and smectic phases are shown in Table I. For each substance, a change in slope of the density vs. temperature plot occurs near the phase transition temperatures. This change in slope clearly indicates that the material being studied changes its method of intramolecular packing at the changes in state. Gabrielli and Verdini⁵ report the density of the liquid crystalline compound, cholesteryl benzoate, over the temperature range from 170 to 200°C. Their results show a negative temperature coefficient of density, with the coefficient greater in the cholesteric phase, $T < 175^{\circ}\text{C}$, than it is in the isotropic phase. Density measurements of CO, CL, CLn and the mixtures in this work are in qualitative agreement with those on cholesteryl benzoate. Gabrielli and Verdini⁵ did not observe an abrupt change of slope of the ρ vs. T curve at T_{IC} . However, their experimental uncertainty was sufficiently great to mask such a change if it

TABLE I
Density and velocity temperature coefficients of CO, CL, CLn, 80% CL-20% CO, and 80% CLn-20% CO.

Sample	ISOTROPIC			CHOLESTERIC			SMECTIC		
	$\Delta v/\Delta T$ ($\text{ms}^{-10} \text{C}^{-1}$)	$\Delta\rho/\Delta T$ ($10^{-4} \text{gm cm}^{-30} \text{C}^{-1}$)	$\Delta v/\Delta T$ ($\text{ms}^{-10} \text{C}^{-1}$)	$\Delta\rho/\Delta T$ ($10^{-4} \text{gm cm}^{-30} \text{C}^{-1}$)	$\Delta v/\Delta T$ ($\text{ms}^{-10} \text{C}^{-1}$)	$\Delta\rho/\Delta T$ ($10^{-4} \text{gm cm}^{-30} \text{C}^{-1}$)	$\Delta v/\Delta T$ ($\text{ms}^{-10} \text{C}^{-1}$)	$\Delta\rho/\Delta T$ ($10^{-4} \text{gm cm}^{-30} \text{C}^{-1}$)	$\Delta\rho/\Delta T$ ($10^{-4} \text{gm cm}^{-30} \text{C}^{-1}$)
CO	4.0	-8.3	-6.9	9.4	-	-9	-	-	-
CL	4.0	-8.3	-6.9	-13	-	-	-4.8	-	-
CLn	4.0	-8.3	-6.9	-13	-	-8.3	-4.8	-	-
80% CL-20% CO	4.0	-8.3	-6.9	-13	-	-	-4.8	-	-
80% CLn-20% CO	4.0	-8.3	-6.9	-13	-	-10	-4.8	-	-

did occur. To the authors' knowledge, no other density studies at the smectic-cholesteric or the cholesteric-isotropic transition have been carried out.

The change of density with temperature for the nematic and isotropic phases of *p*-azoxyphenetole has been studied by Bauer and Bernamont⁶. They reported that at the nematic-isotropic transition, a discontinuity in density exists, i.e. $\Delta\rho/\rho = 0.006$, which can be associated only with a true phase of first order and not a Curie point or second order transition. Gabrielli and Verdini⁵ also report a 0.6% density discontinuity at the nematic-isotropic transition of *p*-azoxyanisole. The discontinuity reported by Bauer and Bernamont⁶ is fourteen times smaller than that which they observed at the solid-nematic transition implying that the increase in molecular separation which occurs at the nematic-isotropic transition is less than that which occurs at the crystal-nematic transition. In this present study, if a step discontinuity in density occurs at the cholesteric-isotropic transition, it is less than 0.1% (limit of uncertainty in reported density values), and thus smaller than that found in the case of the nematic-isotropic transition of *p*-azoxyphenetole.

Figure 3 shows that the density curve for the mixture of 80% CL-20% CO at any temperature falls between those of CL and CO taken alone. On the other hand, Figure 4 shows that the density curve for the mixtures of 80% CLn-20% Co lies above those for the pure components. The latter case indicates that the molecules of CLn and CO in the mixture are capable of closer packing than the molecules of the pure components taken alone.

Relaxation mechanisms

The classical theory of sound propagation in isotropic liquids predicts that the attenuation parameter α/f^2 is a function of the shear viscosity, η_s , and density, ρ_0 , of the medium and the velocity of propagation v . $(\alpha/f^2)_{\text{class}} = 8\pi^2 \eta_s / 3\rho_0 v^3$. On the basis of low shear rate, falling ball viscosity alone $(\alpha/f^2)_{\text{class}}$ for CO and for CL amount to only 25% of α/f^2 measured for the two compounds at 10 MHz. The difference between the measured absorption coefficient, α , and the classical value, α_{class} , is termed the "excess" absorption and must be accounted for by other attenuation mechanisms. Lamb⁷ defines a volume viscosity

$$\eta_v = \frac{4}{3}\eta_s \frac{\alpha - \alpha_{\text{class}}}{\alpha_{\text{class}}} \quad (1)$$

and states that the two major mechanisms responsible for the excess absorption and, hence, η_v are structural and thermal relaxation. Substances whose η_v is ascribed to structural relaxation processes include associated liquids and liquids in which viscoelastic relaxation is observed with shear wave excitation. A volume viscosity related to the thermal processes of rotational and vibrational relaxation

is found in non-associated liquids. Differentiation between structural and thermal relaxation can be made on the basis of the temperature dependence of the ratio η_v/η_s . The temperature dependence of η_v/η_s for CL is similar to that of CLn, CL, and all binary mixtures. The ratio of bulk to shear viscosity for cholesteryl linoleate is 0.8 at 52°C and 0.2 at 37.5°C. Thus, the ratio changes by a factor of four for a temperature change of only 14.5°C. This is considerably greater than changes observed in liquids in which structural relaxation occurs. Lamb⁷ has found that this ratio of viscosities is sensibly temperature-independent and is rarely higher than 20 or less than 0.1 in the case of structural relaxation. For example, η_v/η_s for such diverse liquids as ethanediol, water and mercury change by only approximately 10% for temperature changes of 60°C.

Litovitz and Davis⁸ report that in all liquids thus far investigated ultrasonically, both the shear viscosity and the volume viscosity due to structural relaxation processes increase with decreasing temperature and exhibit nearly the same temperature dependence. They interpret this to mean that the activation enthalpy for shear and structural flow are close in value for most liquids. In CL both η_v and η_s increase as temperature decreases toward T_{IC} ; however, η_s does so at a greater rate. Hence, molecular processes for volume viscosity appear to differ from those controlling shear viscosity.

Lamb⁷ has found that for liquids in which thermal relaxation plays the important role, there is no obvious correlation between the temperature dependence of η_v and η_s . Lack of correlation of the temperature dependence of η_v and η_s in CL in the isotropic phase above T_{IC} indicate that thermal relaxation processes may be significant. One cannot, however, rule out the possibility of contributions to the total absorption from structural relaxation processes as well. In the vicinity of a phase transition, it is likely that both structural and thermal relaxation processes occur in the compounds studied in this work.

Thermal relaxation processes may be inferred also from knowledge of the extreme sensitivity of structure of cholesteric esters to temperature near the transition temperatures. In the isotropic phase, as was shown above, the cholesteric liquid crystals show short range order effects which, as discussed by De Gennes^{9,10}, are extremely sensitive to thermal fluctuations. Litster and Stinson¹¹ have found that thermal fluctuations in the short range order controlling the degree and orientation of alignment of liquid crystalline materials occur in the isotropic region above the isotropic-nematic transition in MBBA. Contributions to α may also arise from a thermal relaxation process related to that which has been observed in the esters methyl and ethyl formate and methyl and ethyl acetate. Karpovich¹² explained that the acetates and formates can exist in two isomeric forms having negligible volume differences but significant energy differences. The cholesteryl esters studied here are more complicated structurally than the formate and acetate esters, and ultrasonic data over a broader frequency range is needed for a more detailed analysis of absorption mechanisms.

In the isotropic phase just above T_{IC} a molecular equilibrium may exist between groups of ordered molecules and surrounding unordered molecules. In structural relaxation, a pressure increase causes a partial conversion of the liquid to a more compact local molecular arrangement. Just above T_{IC} , however, the increased pressure results in an increased temperature which, since thermal fluctuations effect the state of local order, opposes the ordering influence of the pressure increase. Botch and Fixman¹³ have shown that in the neighborhood of a gas-liquid critical point, at which long-range density fluctuations may occur, changes in structure which are significant for ultrasonic experiments can result directly from oscillations of temperature. Hence, it may not be appropriate to explain the process responsible for sound absorption in the isotropic region above T_{IC} as either structural or thermal relaxations but rather as a relaxation which combines both structural and thermal effects.

Figures 7 and 8 show the frequency dependence of α/f^2 and ν , respectively, for CL at several temperatures corresponding to isotropic, cholesteric and smectic phases. The single relaxation frequency relationship $\alpha/f^2 = A/[1 + (f/f_c)^2] + B$ does not fit the experimental data in Figure 7. A summation of two or more relaxation mechanisms is necessary to obtain a fit of the data. Figure 8 shows the characteristic multiple relaxation behavior of velocity.

Comparisons with cholesteryl caprate

In Figure 15 attenuation coefficient measurements taken at 10, 30 and 50 MHz

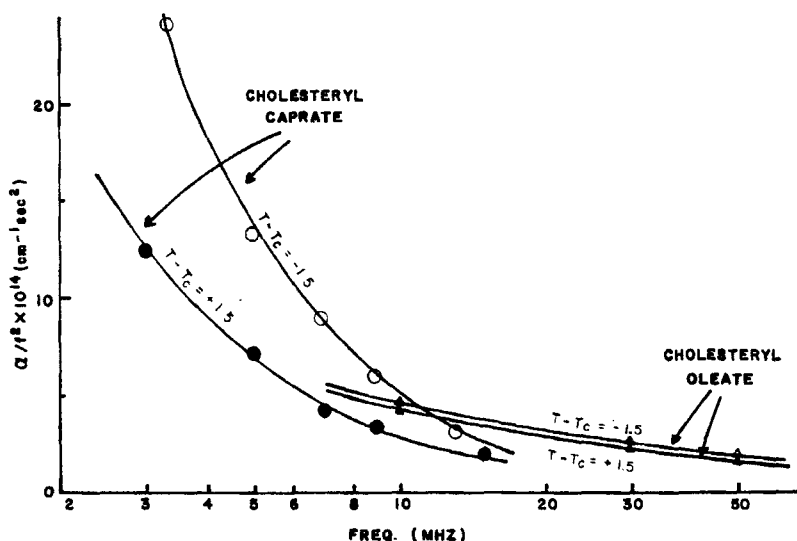


FIGURE 15 α/f^2 vs. frequency for cholesteryl caprate and cholesteryl oleate.

on CO and the results of Zvereva and Kapustin¹⁴ on cholesteryl caprate from 3 to 15 MHz are displayed. A smaller but structurally similar molecule, cholesteryl caprate has a ten carbon saturated fatty acid chain. The temperatures at which measurements are reported are 1.5°C above and below T_{IC} which for cholesteryl caprate is 89.5°C and for cholesteryl oleate is 43.8°C. Zvereva and Kapustin¹⁴ ascribe the observed relaxation phenomena to a relaxation related to the isotropic-cholesteric transition. The process of ultrasonic absorption is associated with a reorientation of the molecular groups in the ultrasonic field. The caprate data suggest the presence of a relaxation whose relaxation frequency must lie above that characterizing the behavior of cholesteryl oleate. The oleate curves indicate that the present data were taken at frequencies that are at the high frequency end of a relaxation region. The observation is consistent with expectations based upon the relative size of the two molecules studied. The caprate ester of cholesterol differs from the oleate ester by its shorter chain length and its degree of saturation.

Phase transition phenomena

Longitudinal wave measurements show no anomalous behavior in either α/f^2 or in ν in the phase transition regions (see Figures 5, 6, 9–14). This result is in apparent disagreement with that of Zvereva and Kapustin¹⁴ on cholesteryl caprate and Hoyer and Nolle¹⁵ on cholesteryl benzoate. For both cholesteryl caprate and benzoate a maximum in the attenuation coefficient and a decrease in velocity have been observed near the isotropic-cholesteric transition. Cholesteryl benzoate was studied at 0.5 MHz and cholesteryl caprate in the range 2.3 to 14.9 MHz. All frequencies, with the one exception of 14.9 MHz, are lower than those available in this present work. Zvereva and Kapustin¹⁴ found that as the measurement frequency increased, the absorption at T_{IC} decreased, such that at 14.9 MHz the existence of a maximum is questionable. Because the cholesteric esters studied in this work are larger than either the cholesteryl caprate or benzoate, it is reasonable to suggest that if a maximum in absorption coefficient occurs it does so at frequencies below 10 MHz.

Measurements of α and ν on the binary mixture of 95% CL-5% CO in the vicinity of T_{IC} reveal no anomalies. This mixture, from Small's¹⁶ binary phase diagram of CO and CL, appears to be a critical concentration at which the phase boundary exhibits a minimum. In this work, measurements of T_{IC} for binary mixtures of CO and CL show that there does not appear to be a minimum in the phase boundary, as indicated by Small's results¹⁶; rather, there appears to be a continuous increase in T_{IC} as the binary mixture changes from pure CL, through the mixtures, to pure CO. Therefore, the absence of anomalous behavior in α and ν is consistent with the characteristics of the phase boundary as observed in this work.

Longitudinal wave velocity

The velocity of propagation of longitudinal waves is expressed in terms of the density and compressibility β_S ,

$$v = \sqrt{\frac{1}{\rho\beta_S}} = \sqrt{\frac{\gamma}{\rho\beta_T}}$$

where β_S and β_T are the adiabatic and isothermal compressibilities, respectively, and γ is the ratio of specific heats, C_p/C_V .

In any one phase, all substances studied have the same temperature coefficient of velocity (Figures 10, 12, 14). Since the temperature coefficients of both v and ρ are negative and from the relationship in Eq. 2, β_S must have a positive temperature coefficient. This result is in qualitative agreement with the work of Gabrielli and Verdini⁵ on cholesteryl benzoate.

Acknowledgement

This work was supported by the National Sciences Foundation, Grant GK-1964. One of us, Joseph F. Dyro, was supported during this work by the National Institute of Health Training Grant 5 TO1 GM-00606 from the National Institute of General Medical Sciences and by Research Grant 5 RO1 HL 01253 from the National Heart and Lung Institute. Joseph F. Dyro thanks Dr. John G. Berberian for kind advice. Mr. Dennis A. Silage was generous with his help in circuit design and data reduction.

References

1. Dyro, J. F. and Edmonds, P. D. *Mol. Cryst. Liquid Cryst.* (to be published in this journal).
2. Edmonds, P. D. and Orr, D. A., *Mol. Cryst.* **2**, 135 (1966).
3. Edmonds, P. D. *Rev. Sci. Instrum.* **37**, 367 (1966).
4. Pellam, J. R. and Galt, J. K. *J. Chem. Phys.* **13**, 608 (1946).
5. Gabrielli, I. and Verdini, L. *Nuova Cim.* (series 10) **2**, 526 (1955).
6. Bauer, E. and Bernamont, J. *J. Phys. Rad.* **7**, 19 (1936).
7. Lamb, J. Thermal Relaxation in Liquids—Chapter 4 in *Physical Acoustics IIA*, Mason, W. P., ed., New York, Academic Press, 1965.
8. Litovitz, T. A. and Davis, C. H. Chapter 5 in Mason, W. P., *Physical Acoustics IIA*, New York, Academic Press, 1965.
9. De Gennes, P. G. *Phys. Lett.* **30A**, 454 (1969).
10. De Gennes, P. G. *Mol. Cryst. Liquid Cryst.* **12**, 193 (1971).
11. Litster, J. D. and Stinson, T. W. *Phys. Rev. Lett.* **25**, 570 (1970).
12. Karpovich, J. *J. Chem. Phys.* **22**, 1767 (1954).
13. Botch, W. and Fixman, M. *J. Chem. Phys.* **42**, 199 (1965).
14. Zvereva, G. E. and Kapustin, A. P. *Soviet Physics (Acoustics)*, **10**, 97 (1964).
15. Hoyer, W. A. and Nolle, A. W. *J. Chem. Phys.* **24**, 803 (1956).
16. Small, D. M. in *Surface Chemistry of Biological Systems*, Plenum Press, New York, 1970, p. 55.